Published in final edited form as:
Nucl Med Biol. 2012 November ; 39(8): 1128–1136. doi:10.1016/j.nucmedbio.2012.06.013.

[^{11}C]Rhodamine-123: synthesis and biodistribution in rodents

Xiaofeng Bao, **Shuiyu Lu**, **Jeih-San Liow**, **Cheryl L. Morse**, **Kacey Anderson**, **Sami S. Zoghbi**, **Robert B. Innis**, and **Victor W. Pike**[1]
Molecular Imaging Branch, National Institute of Mental Health, National Institutes of Health, Bethesda, MD, 20892, USA

Abstract

Introduction—Rhodamine-123 is a known substrate for the efflux transporter, P-glycoprotein (P-gp). We wished to assess whether rhodamine-123 might serve as a useful substrate for developing probes for imaging efflux transporters in vivo with positron emission tomography (PET). For this purpose, we aimed to label rhodamine-123 with carbon-11 ($t_{1/2}$ = 20.4 min) and to study its biodistribution in rodents.

Methods—[^{11}C]Rhodamine-123 was prepared by treating rhodamine-110 (desmethyl-rhodamine-123), with [^{11}C]methyl iodide. The biodistribution of this radiotracer was studied with PET in wild-type mice and rats, in efflux transporter knockout mice, in wild-type rats pretreated with DCPQ (an inhibitor of P-gp) or with cimetidine (an inhibitor of organic cation transporters; OCT), and in P-gp knockout mice pretreated with cimetidine. Unchanged radiotracer in forebrain, plasma and peripheral tissues was also measured ex vivo at 30 min after radiotracer administration to wild-type and efflux transporter knockout rodents.

Results—[^{11}C]Rhodamine-123 was obtained in 4.4% decay-corrected radiochemical yield from cyclotron-produced [^{11}C]carbon dioxide. After intravenous administration of [^{11}C]rhodamine-123 to wild-type rodents, PET and ex vivo measurements showed radioactivity uptake was very low in brain, but relatively high in some other organs such as heart, and especially liver and kidney. Inhibition of P-gp increased uptake in brain, heart, kidney and liver, but only by up to twofold. Secretion of radioactivity from kidney was markedly reduced by OCT knockout or pretreatment with cimetidine.

Conclusions—[^{11}C]Rhodamine-123 was unpromising as a PET probe for P-gp function and appears to be a strong substrate of OCT in kidney. Cimetidine appears effective for blocking OCT in kidney in vivo.

Keywords

[^{11}C]rhodamine-123; P-gp substrate; organic cation transporter; synthesis; carbon-11; PET

1. Introduction

Efflux transporters at blood-organ membrane barriers, such as the blood–brain barrier (BBB), are recognized to strongly influence the biodistribution of drugs, and may pose serious obstacles to effective therapy in conditions such as cancer and HIV infection [1].

[1]Corresponding author: Molecular Imaging Branch, National Institute of Mental Health, National Institutes of Health, 10 Center Drive, Bethesda, Maryland 20892-1003, USA. Tel: + 301 594 5986; fax +301 480 5112., pikev@mail.nih.gov.

Equally, such transporters may influence the biodistribution of diagnostic or imaging tracers and govern whether they are effective for their intended purposes or not [2]. Consequently, the study of efflux transporters with positron emission tomography (PET), especially of P-glycoprotein (P-gp) at the BBB, now gains considerable attention. Several radiotracers have been developed for this purpose [3,4], including [^{11}C]verapamil [5] and [^{11}C]desmethyl-loperamide ([^{11}C]dLop) [6] which are avid substrates for P-gp. These radiotracers are useful for measuring decreased P-gp function as an increase in brain uptake. However, the brain uptake of these radiotracers under normal conditions is so low that any reduction in uptake as a result of increased P-gp function would not be measureable. Therefore, there is a need to develop radiotracers based on less avid substrates that may have measureable moderate brain uptake under normal conditions and that may consequently provide more sensitivity to increased levels of P-gp. PET radiotracers for other efflux transporters, such as BCRP1 (breast cancer resistance protein 1), are also desirable for in vivo investigations [7].

Rhodamine-123 (Chart 1) is a weakly-basic fluorone-based fluorescent dye [8,9]. Intracellular accumulation of rhodamine-123 has been widely used in cancer research to measure P-gp expression responsible for decreased uptake or increased efflux of drugs in resistant cells [10–12]. For example, the ability of cell lines to efflux rhodamine-123 provided a basis for a functional fluorescent assay used by the National Cancer Institute to screen potential anti-cancer drugs for P-gp substrate behavior [13]. Rhodamine-123 has also been used to assess P-gp function at the BBB in mice [14]. Following intravenous infusion of rhodamine-123, concentrations of rhodamine-123 in brain were found to be about 4-fold higher in P-gp knockout (*mdr1a*(−/−)) mice than in wild-type mice. Similarly, rhodamine-123 accumulation in rat brain was increased up to 4-fold upon co-administration with the P-gp inhibitor, cyclosporin A [15]. These data evidence the ability of rhodamine-123 to act as a substrate for P-gp in rodents in vivo. There is one report of rhodamine-123 secretion from isolated perfused rat kidney being mediated by organic cation transporters (OCT) and not by P-gp [16]. Notwithstanding, the efflux transporter substrate selectivity of rhodamine-123 has not been well described.

In this study, we wished to explore whether ^{11}C-labeled rhodamine-123 might provide a useful radiotracer for studying efflux transporters with PET. We describe the labeling of rhodamine-123 with carbon-11 ($t_{1/2}$ = 20.4 min) and our findings on the biodistribution of radioactivity following administration of [^{11}C]rhodamine-123 to rats and to wild-type and efflux transporter knockout mice.

2. Results and Discussion

2.1. Synthesis of [^{11}C]rhodamine-123

[^{11}C]Rhodamine-123 was prepared in an ‘autoloop apparatus’ [17] by treating rhodamine-110 (desmethyl-rhodamine-123 monohydrochloride) with [^{11}C]methyl iodide in the presence of *tetra*-butylammonium hydroxide (TBAH) in *N,N*-dimethylformamide (DMF) (Figure 1) and after HPLC separation and formulation was obtained ready for intravenous injection in 4.4 ± 1.7% (n = 20) decay-corrected radiochemical yield from cyclotron-produced [^{11}C]carbon dioxide. Inefficient trapping of [^{11}C]methyl iodide in the reaction loop mainly accounted for the low yield. Radiolabeled product was identified by co-elution with reference rhodamine-123 in analytical reverse phase HPLC (t_R = 5.6 min) and by LC-MS/MS of associated carrier (LC-MS, $[M+H]^+$ = 345.4, and LC-MS/MS, $[M–COOMe]^+$ = 285.3, $[M–OMe]^+$ = 313.5, $[M–NH_2]^+$ = 328.2). Furthermore, treatment of labeled product with aqueous KOH produced a new radioactive compound eluting at the solvent front (2.4 min) on analytical reverse phase HPLC, consistent with ester hydrolysis of [^{11}C]rhodamine-123 to [^{11}C]methanol. The radiosynthesis required only 35 min and the activities of [^{11}C]rhodamine-123 produced in the final dose for injection averaged 877 ± 241

MBq (n = 20). These activity levels were fully adequate for our subsequent experiments and therefore no attempts were made to further improve isolated yields. The radiochemical purities of doses of [^{11}C]rhodamine-123 exceeded 99%.

[^{11}C]Rhodamine-123 was well separated with HPLC from rhodamine-110 and other impurities. Thus, chemical impurities were estimated to be less than 1 nmol per batch when impurities were assumed to have the same extinction coefficient at 254 nm as rhodamine-123. The average specific radioactivity of [^{11}C]rhodamine-123 was 13.4 ± 4.4 GBq/μmol (n = 20) at the end of synthesis. This value is much lower than for other ^{11}C-labeled radiotracers produced in our laboratory from [^{11}C]methyl iodide. This relatively low specific radioactivity was due to rhodamine-123 impurity in the purchased rhodamine-110 precursor (99% pure), as we discovered by reverse phase HPLC analysis of the starting material. However, high specific radioactivity would not be required for this radiotracer because it is not targeted at imaging a saturable binding site. Therefore, the precursor was not further purified for this study. [^{11}C]Rhodamine-123 was radiochemically stable (99.0 ± 0.9% unchanged, n = 4) for at least 1 h in sterile saline or for at least 2.5 h in sodium phosphate buffer (0.15 M) at room temperature.

2.2. Rhodamine-123 lipophilicity

For compounds of low molecular weight (< 450 Da) and low polar surface area (PSA; < 90 Å^2), such as rhodamine-123 (m.wt., 344 Da; PSA, 85 Å^2), lipophilicity is expected to be the major property determining ability to cross the BBB or other lipophilic membranes by passive diffusion [18]. We found the log of the distribution coefficient of [^{11}C]rhodamine-123 between n-octanol and pH 7.4 buffer at room temperature (log$D_{7.4}$) to be 0.85 ± 0.01 (n = 6). Lampidis et al. obtained a similar value (0.53) for rhodamine-123 with spectrophotometry [19]. The log$P$ value for the neutral species has been found to be 1.06 ± 0.06 [20]. The true pK_a of rhodamine-123 has been measured through the pH-dependence of its fluorescence [20]. Calculation of the log$D_{7.4}$ value from the true log$P$ and pK_a (7.2) by correction with the Henderson-Hasselbach equation [i.e., log$D_{7.4}$ = log$P$–log(1 + $10^{(7.4 - pKa)}$)] gives a value of 0.65, which, although lower, also quite closely agrees with our measured value. This calculation assumes that protonated rhodamine-123 is unable to enter the n-octanol phase because of its positive charge. This assumption is however false for rhodamine-123. Thus, the intrinsic partition coefficient P_i for the protonated species between aqueous phase and n-octanol has been found to be almost identical to that of the neutral species P_u, with the ratio $\alpha = P_i/P_u = 1.004 \pm 0.090$ [20]. The large spatial intramolecular delocalization of charge likely mitigates the effect of protonation on solubility in n-octanol [21]. The delocalization of charge is verified in the X-ray structure, which is symmetric with equal length C–N bonds that evince partial double bond character [22].

Water and n-octanol have considerable mutual solubility which may influence the distribution of drugs between these two phases. Water and cyclohexane are mutually insoluble and drug partition coefficients are often also measured between these two solvents. We measured the distribution coefficients of [^{11}C]rhodamine-123 between cyclohexane and buffers (D_{cyclo}) in the pH range 4.5–10, which spans the measured pK_a value (7.2). [^{11}C]Rhodamine-123 was remarkably insoluble in the cyclohexane phase across the whole of this pH range (logD_{cyclo}, < −2.9).[2] Furthermore, the dependence of logD_{cyclo} on pH was very weak and did not reveal an apparent pK_a (Figure 2). The pH-dependence of log$D$ between buffer and n-octanol similarly fails to reveal the pK_a [20]. Figure 2 confirms that

[2]Rhodamine-123 is often described in the literature as a ‘lipophilic cation’. However, the experimental data show this description to be a double misnomer, because rhodamine-123 is neither lipophilic with log$P$ < 1, nor predominantly cationic at physiological pH (7.4) with a pKa value of 7.2.

the neutral and protonated forms of rhodamine-123 are very weakly hydrophobic, and conversely highly hydrophilic, to an almost equal extent. These properties may clearly impact on the biodistribution of rhodamine-123, and in particular on the ability of this compound to diffuse across lipophilic membranes, such as the BBB.

2.3. Plasma free fraction

The extent to which a drug is free in plasma (i.e., not bound to plasma proteins) has an important influence on pharmacokinetics and biodistribution. Plasma free fractions of [^{11}C]rhodamine-123 in mouse and rat blood were found to be 0.156 ± 0.007 (n = 3) and 0.090 ± 0.004 (n = 3), respectively. By contrast, De Lange et al. [14] found an appreciably higher free fraction in mouse (0.23 ± 0.04) by use of a non-radiometric method. In view of the hydrophilicity of rhodamine-123, the plasma free fraction is perhaps lower than might be expected [23]. This may again reflect an ability of the protonated species to interact with hydrophobic entities, including hydrophobic domains in plasma proteins.

2.4. PET imaging of [^{11}C]rhodamine-123 in rodents

2.4.1. Low sustained uptake in brain increased by DCPQ—After intravenous injection of [^{11}C]rhodamine-123 into rats, the uptake of radioactivity measured with PET in whole brain peaked early (< 1 min) but at a very low value (< 0.27 SUV) (Figure 3). In mouse, the pattern and magnitude of radioactivity uptake in brain resembled that in rat (Figure 3). Rats injected with [^{11}C]rhodamine-123 after treatment with the P-gp inhibitor, DCPQ [24] ((2*R*)-*anti*-5-{3-[4-(10,11-dichloromethanodibenzosuber-5-yl)piperazin-1-yl]-2-hydroxypropoxy}quinoline trihydrochloride) (32 mg/kg, i.v.), showed up to twofold increase in radioactivity uptake and retention in brain (Figure 3). This result suggests that rhodamine-123 is excluded from untreated brain by the action of P-gp at the BBB, in accord with previous data obtained in rodents in vitro and in vivo [14,15]. Clearly, even when P-gp was inhibited, uptake of radioactivity into rat brain after [^{11}C]rhodamine-123 administration was still very low (< 0.6 SUV). This is probably because the low intrinsic lipophilicities of the neutral rhodamine-123 species and of its protonated form disfavor free diffusion across the BBB. Such very low uptake, even under P-gp inhibited conditions, would preclude [^{11}C]rhodamine-123 from serving as a valuable PET probe of BBB P-gp function.

The decay-corrected time-activity curves for rodent brain from both baseline and DCPQ-pretreatment experiments are characterized as having fast initial radioactivity uptake followed by washout over 30 minutes down to a constant level (Figure 3). PET, because it measures radioactivity only, is unable to inform on the radioactive species being detected. These species may include parent radiotracer and possible radiometabolites [2]. Moreover, PET has limited spatial resolution (~ 2 mm) and consequently is unable to inform on the distribution of radioactivity between different compartments in each voxel being measured. In human, blood composes about 4% of brain volume, and this is expected to be similar in rodents. Therefore, in the very early phase of the PET time-activity curves for brain, a significant proportion of measured radioactivity may represent that in blood. Rhodamine-123 is known to be very rapidly cleared from rat blood [25], and hence the contribution of blood radioactivity to PET measurements of total radioactivity in rodent brain is expected to decrease rapidly with scan progress. Radioactivity remaining in brain in the late phase of scanning may be composed of parent radiotracer and/or radiometabolites. We measured ex vivo the radioactive species in rodent organs at 30 min after administration of [^{11}C]rhodamine-123. The results of these experiments (Tables 1 and 3) are later discussed in more detail; essentially, they showed that the very low radioactivity in forebrain has an appreciable radiometabolite component (32% in rat and 18% in mouse).

In the PET experiment, the lack of washout of radioactive species from brain after about 30 min from radiotracer administration indicates operation of a trapping mechanism (Figure 3). The weak base and P-gp substrate, [^{11}C]dLop, shows similar stability for decay-corrected time-activity curves in rodent, monkey and human brain, and in this case the lack of washout has been identified as entrapment within acidic lysozymes due to radiotracer protonation [26]. However, rhodamine-123, despite being a weak base with a pK_a almost identical to that of dLop (pK_a, 7.2–7.3) [6], does not trap in acidic lysozomes [20]. A likely explanation is that the neutral form of rhodamine-123 is simply inadequately lipophilic (log$D$ < 1) to cross lysozomal membranes (unlike dLop with log$D$ = 2.60; [23]). By contrast, rhodamine-123 is well-known to accumulate in mitochondria [20], putatively as the cation, due to the strong negative electrical potential (−150 to −170 mV) of the mitochondrial membrane [27]. For this reason, rhodamine-123 can be used as a selective mitochondrial stain in living cells [28]. Mitochondria are therefore likely to be responsible for entrapping low amounts of [^{11}C]rhodamine-123 in brain.

2.4.2. Moderate uptake in whole heart increased by DCPQ—Uptake of radioactivity in rat or mouse whole heart following intravenous administration of [^{11}C]rhodamine-123 was several-fold higher than in brain throughout scanning (Figure 3). In both species the decay-corrected time-activity curves showed a very early peak, which then quickly declined to much lower stable levels. The PET scanning in these small animals is unable to discriminate myocardium from blood in heart chambers, because of limited resolution. Hence, radioactivity in blood most likely contributed heavily to the early spike in measured radioactivity. A previous study gave unlabeled rhodamine-123 (18 μg) as bolus intravenous injections to mice and with ex vivo measures found high accumulation of rhodamine-123 in heart muscle at 30 min which was sustained beyond 24 h [29]. In the same study, clearance of rhodamine-123 from blood was rapid such that the heart to blood concentration ratio became very high (~ 90 at 24 h) [29]. Prolonged retention of rhodamine-123 by cardiac muscle mitochondria has also been observed in vitro [30]. Thus, the moderately high and stable levels of radioactivity seen in the PET time-activity curves preponderantly represent radioactivity in myocardial tissue (Figure 3). Ex vivo measurements showed that radioactivity in mouse myocardium was over 97% unchanged radiotracer at 30 min after administration of [^{11}C]rhodamine-123 (Table 3).

DCPQ-pretreatment of the rats appreciably increased radioactivity uptake into heart. Human and rodent cardiomyocytes are well-known to express P-gp [31,32], and inhibition of P-gp is likely responsible for the increased heart uptake in DCPQ-pretreated rats. Some caution is however required before decisively attributing the effect of DCPQ solely to inhibition of P-gp, because the full effect of DCPQ on the availability of free [^{11}C]rhodamine-123 in blood throughout scanning was unknown. However, ex vivo measurements at 30 min after radiotracer injection showed lower [^{11}C]rhodamine-123 concentration in the plasma of DCPQ-treated rats than in untreated rats (Table 2), so indicating that a lower input of radiotracer gave a higher uptake into heart. This further supports the interpretation that P-gp is involved in inhibiting the heart uptake of [^{11}C]rhodamine-123. Radioactive derivatives of rhodamine-123, such as radiofluorinated fluoroethylrhodamine B (Chart 1), have been considered as possible PET radiotracers of myocardial perfusion [33]. Thus, the organ uptake of [^{11}C]rhodamine-123 might be perfusion-dependent. Whether DCPQ did affect perfusion was not however investigated in this study.

2.4.3. High uptake in kidney and evidence for OCT substrate behavior—Time-activity curves for radioactivity uptake in kidney following intravenous administration of [^{11}C]rhodamine-123 to rats or mice, in striking contrast to those for brain and heart, showed an early high peak uptake followed by a slow progressive decline in radioactivity

concentration (Figure 4). The specific mechanism responsible for the high radioactivity uptake in kidney is unclear.

P-gp is expressed in rodent kidney and rhodamine-123 has been used to assess kidney P-gp function in vivo [34]. The selective P-gp inhibitors, cyclosporin A and digoxin, have been reported not to influence the secretion of rhodamine-123 from kidney [16]. In this study, treatment of rats with DCPQ before [^{11}C]rhodamine-123 administration resulted in even greater peak uptake of radioactivity in kidney without grossly changing the shapes of the time-activity curves (Figure 4). These results appear consistent with P-gp acting as an efflux transporter that resists uptake of rhodamine-123 into kidney. Nonetheless, similar reservations apply to the interpretation of the kidney PET data, as to the brain and heart PET data. Thus, PET measurements of radioactivity in the kidney region of interest will derive from the sum of the radioactivity in kidney tissue, blood and tubular urine in each measured voxel. In this regard, the contribution of tubular urine is unknown. Ex vivo measurements showed that 99% of radioactivity in mouse kidney tissue was unchanged radiotracer at 30 minutes after administration (Table 3) and also that the ratio of kidney tissue to plasma (or whole blood) radioactivity was exceptionally high (Table 4, Figure 7), as was the ratio of total radioactivity in kidney to that in whole blood (~ 50). Hence, circulating blood and radiometabolites likely contributed little to radioactivity measurements in kidney. As mentioned previously, DCPQ lowered the concentration of [^{11}C]rhodamine-123 in plasma at 30 min after radiotracer administration (Table 2). The higher level of radioactivity in kidney under DCPQ-treated conditions was therefore unlikely due to greater availability from blood.

A single report has indicated that other efflux transporters, the organic cation transporters (OCT), secrete rhodamine-123 from isolated perfused rat kidney [16]. Cimetidine is considered to be an inhibitor of OCT but not of P-gp [16]. Rats pretreated with cimetidine before administration of [^{11}C]rhodamine-123 showed slightly lower peak radioactivity in kidney followed by a distinctly slower decline in radioactivity than untreated rats, whereas time-activity curves for brain and heart showed virtually no differences between untreated and cimetidine-treated rats (Figure 5). As this effect of cimetidinewas specific to kidney, this finding appears to be due to OCT inhibition rather than to any other possible effect of cimetidine, such as alteration of blood flow or free radiotracer concentration in blood. These results therefore indicate that cimetidine is an effective inhibitor of OCT in vivo.

In order to further elucidate the role of OCT in kidney, we used PET to compare the washout of [^{11}C]rhodamine-123 from four different groups of mice, namely wild-type, P-gp knockout, cimetidine-pretreated P-gp knockout, and Oct1/2 knockout mice (Figure 6). The time-activity curves for P-gp knockout and wild-type mice were virtually identical (c.f., left and right panels, Figure 6). These results argue against a significant involvement of P-gp in either the uptake or secretion of rhodamine-123 from kidney, unlike the aforementioned findings in DCPQ-treated rats (Figure 4). By contrast the Oct1/2 knockout mice showed a markedly different time-activity curve to wild-type or P-gp knockout mice, with a significantly lower peak radioactivity, followed by a distinctly slower washout of radioactivity (Figure 6). Peak uptake of radioactivity in kidney in cimetidine-pretreated P-gp knockout mice was markedly lower than in untreated P-gp knockout mice, and was followed by slow accumulation of radioactivity (Figure 6). Therefore, cimetidine appreciably suppressed kidney radioactivity level in mice as in rats. Time-activity curves in Oct1/2 knockout mice quite strongly resembled those in cimetidine-pretreated P-gp knockout mice. Ex vivo analyses of radioactivity in kidney tissue at 30 min after administration to wild-type, P-gp knockout and Oct1/2 knockout mice showed that this radioactivity was > 97% unchanged radiotracer (Table 3). As stated previously, rhodamine-123 is known to be cleared from blood very rapidly, and our ex vivo measures showed that the ratio of

radioactivity concentration in kidney tissue to that in plasma was > 1000 at 30 min after radiotracer administration (Table 4, Figure 7). Therefore, blood negligibly contaminated the PET measures in mouse kidney. These PET data bolster the evidence for rhodamine-123 acting as a substrate for OCT in kidney.

2.4.4. High uptake in liver increased by DCPQ—Rat liver is known to metabolize rhodamine-123, mainly to its glucuronide [25]. Time-activity curves for radioactivity in liver following intravenous administration of [^{11}C]rhodamine-123 to rats or mice showed an early high peak followed by a slow decline (Figure 4).

P-gp is expressed in liver and has been found to dispose of rhodamine-123 from liver into bile [34]. In liver, although the efflux transporter, MRP2, has no action on rhodamine-123 it does dispose of the glucuronide metabolite [35]. The selective P-gp inhibitor cyclosporin A substantially decreases the biliary excretion of rhodamine-123 from isolated perfused rat liver [35] and inhibition of rhodamine-123 secretion by cyclosporin A has been suggested as a model of P-gp–mediated liver transport [36]. Pretreatment of rats with DCPQ resulted in greater peak radioactivity in liver, without any gross change in the shape of time-activity curves (Figure 4). These results appear consistent with the previously reported action of P-gp in disposing of rhodamine-123 from liver.

2.5. Ex vivo measurement of radiometabolites and distribution of [^{11}C]rhodamine-123 in rat

[^{11}C]Rhodamine-123 was found to be completely stable for at least 2.5 h in rat plasma, whole blood and forebrain homogenates at 37 °C. Therefore, ex vivo measurements of radiotracer were feasible in experiments designed to clarify results from rodent PET imaging.

At 30 min after administration of [^{11}C]rhodamine-123 to rats, reverse phase radio-HPLC of plasma showed the radioactivity to be composed predominantly of unchanged radiotracer (79.7 ± 7.1%; t_R = 11 min) plus two unresolved radiometabolites eluting near the solvent front (between 1.7 and 3.3 min). Rhodamine-123, as well as being converted into its glucuronide in rat liver is also metabolized by hydrolysis to the acid, rhodamine-110 [25]. Therefore, one of the observed radiometabolites is deduced to be the glucuronide. The other relatively polar radiometabolite is probably a one-carbon species arising from demethylation. Such polar radiometabolites and the radioactive glucuronide would be expected to have low ability to cross lipophilic membranes.

At 30 min after administration of [^{11}C]rhodamine-123 to rats, *total* forebrain radioactivity content was slightly higher in DCPQ-pretreated rats (0.068 ± 0.027 SUV) than in untreated (0.061 ± 0.010 SUV) or cimetidine-treated rats (0.048 ± 0.016 SUV). The total plasma radioactivity level was lower in DCPQ-pretreated rats (0.173 ± 0.031 SUV) than in untreated rats (0.362 ± 0.077 SUV) or in cimetidine-pretreated rats (0.445 ± 0.098 SUV) at 30 min after radiotracer injection. Consequently, the ratio of total brain radioactivity to that in plasma was 3.7 fold higher in DCPQ-treated rats than in untreated rats. The radioactivity in forebrain and plasma of each group of rats was predominantly composed of unchanged radiotracer (Table 1). DCPQ-pretreatment decreased the percentage of radioactivity represented by unchanged [^{11}C]rhodamine-123 in plasma whereas cimetidine-pretreatment increased this value. DCPQ likely caused increased exposure of the radiotracer to metabolizing enzymes in liver. By contrast, cimetidine may have protected [^{11}C]rhodamine-123 from metabolism, possibly through its known ability to inhibit P450-mediated pathways [37,38] and/or glucuronidation [39].

Consideration of the absolute concentrations of unchanged radiotracer shows that DCPQ-pretreatment substantially increased the forebrain to plasma ratio at 30 min after radiotracer

injection relative to that in untreated or cimetidine-pretreated rats (Table 2). These data provide further evidence for [^{11}C]rhodamine-123 acting as a P-gp substrate at the rat blood-brain barrier.

2.6. Ex vivo studies of metabolism and distribution of [^{11}C]rhodamine-123 in wild-type and transporter knockout mice

In wild-type mice, at 30 min after [^{11}C]rhodamine-123 injection, only 14.3% of the radioactivity in plasma was unchanged radiotracer, with the remainder mainly represented by two radiometabolites eluting near the solvent front in the radio-HPLC analysis (Table 3). One of these two radiometabolites is likely the glucuronide, as in rat. Concurrent analyses of forebrain, heart and kidney tissue showed that unchanged radiotracer represented high percentages of the total radioactivity and therefore that the relatively polar radiometabolites seen in plasma were well excluded from these organs. Although, the percentage of radioactivity represented by radiometabolites is higher in brain than in heart and kidney (Table 3), this is because the uptake of unchanged radiotracer into brain is lower than in heart or kidney. Radiometabolites were also well excluded from heart and kidney in P-gp, Oct1/2, BCRP (ABCG2) and MRP1 (ABCC1) knockout mice. The majority of radioactivity found in the forebrain of Oct1/2 and BCRP knockout mice was composed of radiometabolites, whereas in P-gp and MRP1 knockout mice parent radiotracer represented the majority of radioactivity, as in wild-type mice.

In all mouse groups, absolute concentrations of unchanged [^{11}C]rhodamine-123 were very low in plasma and forebrain and very high in heart and kidney (Table 4). Values were comparable across mouse groups, except in P-gp knockout mice which showed decreased plasma concentration and increased forebrain concentration relative to those in wild-type mice. Tissue to plasma [^{11}C]rhodamine-123 concentration ratios for kidney, heart and forebrain were appreciably higher in P-gp knockout mice than in other groups (Figure 7), thereby reflecting the action of P-gp on [^{11}C]rhodamine-123 in these organs.

3. Conclusions

The biodistribution of [^{11}C]rhodamine-123 is strongly influenced by physicochemical parameters (i.e., log$D$, α, pK_a) and by the action of P-gp at the BBB and at peripheral organs, and also of OCT in kidney. [^{11}C]Rhodamine-123 is unpromising as a PET probe for the study of P-gp function at the BBB. Structural modifications to rhodamine-123 would be required to deliver promising PET probes for the study of brain efflux transporter function, based on this structural platform.

4. Experimental

4.1 Materials and general methods

All reagents and organic solvents were ACS grade or higher and used without further purification. Iodomethane, ammonium formate, *tetra*-butylammonium hydroxide (TBAH) were purchased from Sigma-Aldrich (Milwaukee, WI). Rhodamine-110 (99%, laser grade) and rhodamine-123 (99%, laser grade) were purchased from Acros Organics (Pittsburgh, PA). Cimetidine was obtained from Sigma-Aldrich. DCPQ was a gift from Eli Lilly & Co (Indianapolis, IN).

LC-MS was performed on a LCQ Deca instrument (Thermo Fisher Scientific Corp.; Waltham, MA) equipped with a reverse-phase HPLC column (Synergi Fusion-RP, 4 μm, 150 mm × 2 mm; Phenomenex, Torrance, CA). The instrument was set up to perform electrospray ionization (spray voltage 5 kV, nitrogen sheath flow 65 units, auxiliary gas flow 10 units, capillary voltage 35 V, and capillary temperature 260 °C). For the characterization

of synthesized compounds, the column was eluted at 150 μL/min, either isocratically or with a gradient between H_2O: MeOH: AcOH (90: 10: 0.5 by vol.) and MeOH: AcOH (100: 0.5 v/v).

High activities of carbon-11 (> 37 kBq) were measured with a calibrated ionization chamber (Atomlab 300; Biodex Medical Systems, Shirley, NY). Low activities of carbon-11 (< 1 kBq) were measured in an automatic γ-counter (model 1480 Wizard; Perkin-Elmer, Boston, MA) with an electronic window set between 360–1800 keV (counting efficiency 51.84%). Measurements of carbon-11 were corrected for any significant background and for physical decay with a half-life 20.4 min.

Sprague-Dawley rats, and wild-type, P-gp knockout, Oct1/2 (organic cation transporter 1 and 2) knockout, BCRP knockout and MRP1 knockout mice were purchased from Taconic Farm (Germantown, NY). All animal experiments were performed in accordance with the Guide for the Care and Use of Laboratory Animals [40] and were approved by the National Institute of Mental Health Animal Care and Use Committee.

4.2. Radiosynthesis of [^{11}C]rhodamine-123

[^{11}C]Iodomethane (~ 40 GBq) was produced from cyclotron-produced [^{11}C]carbon dioxide with a PETtrace MeI Microlab (GE Medical Systems, Milwaukee, WI) apparatus and delivered in helium gas (17 mL/min) into a loop of stainless steel tubing (2 mL; Bioscan, Washington, DC) preloaded with rhodamine-110 (2 mg, 6 μmol) and TBAH (12 μL, 1M in MeOH, 12 μmol) in DMF (80 μL). Reaction was allowed to proceed at room temperature for 5 min, and then the entire contents of the loop were loaded onto a Luna C18 column (250 × 10 mm, 5 μm; Phenomenex) eluted at 6 mL/min with a mixture of aq. $HCOONH_4$ (A, 10 mM) and MeCN (B), with B increased from 40 to 70% over 20 min. [^{11}C]Rhodamine-123 (t_R = 10.3–11.3 min) was collected. Mobile phase was removed under vacuum at 80 °C and the residue was then dissolved in sterile saline (USP grade, 10 mL). The [^{11}C]rhodamine-123 solution was then filtered through a sterile filter (Millex MP, 0.22 μm; Millipore, Bedford, MA). A sample of this product was analyzed for radiochemical purity and specific radioactivity with radio-HPLC on a reverse phase Prodigy column (10 μm, 250 × 4.6 mm; Phenomenex) eluted with a mixture of aq. $HCOONH_4$ (10 mM) and MeCN (55/45, v/v) at 2 mL/min, with eluate monitored for absorbance at 254 nm (Gold 166 detector; Beckman Instruments; Fullerton, CA) and radioactivity (pin diode detector HC-003; Bioscan). The product was identified as [^{11}C]rhodamine-123 (t_R = 5.6 min) by (i) coelution with authentic rhodamine-123 on analytical HPLC, (ii) LC-MS of associated carrier; (iii) LC-MS/MS of associated carrier; and (iv) hydrolysis with saturated KOH (aq.) followed by re-analysis with radio-HPLC. Formulated [^{11}C]rhodamine-123 was kept at room temperature for 1 h and then re-analyzed by radio-HPLC to test radiochemical stability.

4.3. Lipophilicity and free fraction

[^{11}C]Rhodamine-123 was first shown by radio-HPLC analysis to be stable in sodium phosphate buffer (0.15M) at room temperature for at least 2.5 h. We therefore applied a radiometric method for determining radiotracer log$D_{7.4}$, as described previously [23,41]. Briefly six samples of [^{11}C]rhodamine-123 (1.11 MBq; > 99% radiochemical purity) in sodium phosphate buffer (1.0 mL; 0.15 M; pH 7.40) were each extracted into *n*-octanol. Each phase was then measured for radioactivity concentration in a γ-counter. Radioactivities that were initially too high to be measured without incurring significant dead-time errors were left to decay to be within the optimal range of the γ-counter. The samples had counting errors of no more than 0.3 ± 0.0% (n = 6) at one standard deviation. Radioactivity concentration in the aqueous phase was corrected for radiochemical impurity

by radio-HPLC analysis. The log of the decay-corrected ratio of radioactivity concentration in the *n*-octanol phase to the corrected concentration in buffer gave $\log D_{7.4}$.

The pH-dependence of the distribution of [^{11}C]rhodamine-123 between cyclohexane and sodium phosphate buffers (0.15 M) was measured as above but with cyclohexane replacing *n*-octanol. Determinations were made in triplicate without radio-HPLC correction of radioactivity concentration in the aqueous phase.

Plasma free fractions in mice and rats were determined with a published method [42].

4.4. PET imaging of [^{11}C]rhodamine-123 in rodents

All animals were anesthetized with 1.5% isoflurane. Scans were acquired for 90 min with a microPET Focus 220 (rats) or 120 (mice) PET camera (Siemens Medical Solutions; Knoxville, TN). Formulated [^{11}C]rhodamine-123 (~ 150 μL) was injected intravenously through a penile vein catheter for rats (28.9 ± 5.9 MBq) and through a tail vein catheter for mice (18.1 ± 7.4 MBq). In some experiments rodents were administered with DCPQ (32 mg/kg, i.v.), a potent P-gp inhibitor, or cimetidine (30 mg/kg, i.v.), an OCT inhibitor. These agents were administered intravenously at 30 min before radiotracer injection, also via a penile or tail vein catheter. Images were reconstructed using Fourier rebinning followed by 2D filtered back projection with attenuation correction for rats or 2D OSEM without attenuation correction for mice. No scatter correction was applied for mice.

4.5. Rat experiments with ex vivo measurements

Thirteen Sprague-Dawley rats were anesthetized by inhalation of 1.5% isoflurane and administered [^{11}C]rhodamine-123 (38.8 ± 8.0 MBq) intravenously through the penile vein (a) at baseline (i.e., with no drug treatment; $n = 5$); (b) at 30 min after injection of the P-gp inhibitor DCPQ (32 mg/kg i.v.; $n = 3$) or (c) at 30 min after the administration of the OCT inhibitor cimetidine (30 mg/kg, i.v.; $n = 5$). Anticoagulated blood was removed by cardiac puncture to provide plasma for radio-HPLC analysis. Each rat was sacrificed by thoracotomy at 30 min after radiotracer injection. Forebrains were removed, weighed and immediately processed for radio-HPLC analysis.

Plasma was separated from collected blood by centrifugation and measured for radioactivity in an automatic γ-counter, as previously described [43]. Typically, plasma samples (~ 450 μL) were then deproteinized with MeCN (720 μL). The radioactivities of various plasma and forebrain tissues were counted in an automatic γ-counter, and then homogenized in MeCN (1.5 mL) with a hand-held tissue Tearor (model 985–370, BioSpec Products Inc., Bartlesville, OK), followed by homogenization in the presence of water (500 μL). The homogenates were counted again in the γ-counter to enable calculation of the percentage recovery of radioactivity into MeCN extracts. All tissue radioactivity measurements were corrected for physical decay with a half-life of 20.385 min. The homogenates were then centrifuged at 10,000 × g for 1 min. Radioactivities in the resulting precipitates were used to calculate the percentage recovery of activity in the MeCN supernatant liquids. The clear pre-filtered supernatant liquids were analyzed with radio-HPLC on a Novapak® C18 column (4 μm, 100 mm × 8 mm, Waters Corp., Milford, MA) housed in a radial compression module RCM-100, and eluted with MeCN and aq. ammonium formate (10 mM) (60: 40 v/v) at 2.0 mL/min. Eluate was monitored for radioactivity with an in-line flow-through Na(Tl) scintillation detector (Bioscan). Chromatographic data were corrected for physical decay to each chromatogram start time, stored and analyzed by “Bio-Chrom Lite” software (Bioscan).

4.6. Stability of [^{11}C]rhodamine-123

Forebrain and anticoagulated blood were harvested from an anesthetized rat. [^{11}C]Rhodamine-123 (0.488 MBq in 1.2 μL) was incubated with plasma (0.5 mL) or whole blood (0.5 mL) at 37 °C for 2.5 h. [^{11}C]Rhodamine-123 (2.93 MBq in 60 μL) was similarly incubated with forebrain homogenate (5 mL). Incubates were then sampled, deproteinized with MeCN and analyzed with radio-HPLC

4.7. Mice studies with ex vivo measurements

All mice, after being anesthetized with 1.5% isoflurane, were injected intravenously through the tail vein with [^{11}C]rhodamine-123 (13.2 ± 5.9 MBq, n = 19). Anti-coagulated blood was removed by cardiac puncture. Each mouse was then sacrificed by thoracotomy at 30 min after injection of radioactivity. Forebrains, hearts, and kidneys were removed, weighed and immediately subjected to radioanalysis. Plasma was separated from blood by centrifugation. Plasma and tissue samples were quantified for radioactivity, as described above.

Acknowledgments

This research was supported by the Intramural Research Program of the National Institutes of Health (NIMH). We are grateful to the NIH Clinical PET Center (Chief: Dr. Peter Herscovitch) for cyclotron production of carbon-11.

References

1. Ayrton A, Morgan P. Role of transport proteins in drug discovery and development: a pharmaceutical perspective. Xenobiotica. 2008; 38:676–708. [PubMed: 18668427]
2. Pike VW. PET radiotracers: crossing the blood-brain barrier and surviving metabolism. Trends Pharmacol Sci. 2009; 30:431–440. [PubMed: 19616318]
3. Kannan P, John C, Zoghbi SS, Halldin C, Gottesman MM, Innis RB, et al. Imaging the function of P-glycoprotein with radiotracers: pharmacokinetics and in vivo applications. Clin Pharmacol Therapeutics. 2009; 86:368–377.
4. Colabufo NA, Berardi F, Perrone MG, Capparelli E, Cantore M, Inglese C, et al. Substrates, inhibitors and activators of P-glycoprotein: candidates for radiolabeling and imaging perspectives. Curr Topics Med Chem. 2010; 10:1703–1714.
5. Luurtsema G, Molthoff CFM, Schuit RC, Windhorst AD, Lammertsma AA, Franssen EJF. Evaluation of (*R*)-[^{11}C]verapamil as PET tracer of P-glycoprotein function in the blood-brain barrier: kinetics and metabolism in the rat. Nucl Med Biol. 2005; 32:87–93. [PubMed: 15691665]
6. Lazarova N, Zoghbi SS, Hong J, Seneca N, Tuan E, Gladding RL, et al. Synthesis and evaluation of [*N*-*methyl*-^{11}C]*N*-desmethyl-loperamide as a new and improved PET radiotracer for imaging P-gp function. J Med Chem. 2008; 51:6034–6043. [PubMed: 18783208]
7. Dörner B, Kuntner C, Bankstahl JP, Wanek T, Bankstahl M, Stanek J, et al. Radiosynthesis and in vivo evaluation of 1-[^{18}F]fluoroelacridar as a positron emission tomography tracer for P-glycoprotein and breast cancer resistance protein. Bioorg Med Chem. 2011; 19:2190–2198. [PubMed: 21419632]
8. Schäfer, FP., editor. Dye lasers. 3. Berlin: Springer-Verlag; 1990.
9. Duarte, FJ.; Hillman, LW., editors. Dye laser principles. New York: Academic Press; 1990.
10. Canitrot Y, Lautier D. Detection of multidrug-resistance phenotype using rhodamine-123. Bull Cancer. 1995; 82:687–697. [PubMed: 8535026]
11. Wagner-Souza K, Diamond HR, Ornellas MH, Gomes BE, Almeida-Oliveira A, Abdelhay E, et al. Rhodamine 123 efflux in human subpopulations of hematopoietic stem cells: Comparison between bone marrow, umbilical cord blood and mobilized peripheral blood CD34(+) cells. Int J Mol Med. 2008; 22:237–242. [PubMed: 18636179]
12. Perloff MD, Stormer E, von Moltke LL, Greenblatt DJ. Rapid assessment of P-glycoprotein inhibition and induction in vitro. Pharmaceutical Res. 2003; 20:1177–1183.

13. Lee J-S, Paull K, Alvarez M, Hose C, Monks A, Grever M, et al. Rhodamine efflux patterns predict P-glycoprotein substrates in the National Cancer Institute drug screen. Mol Pharmacol. 1994; 46:627–638. [PubMed: 7969041]
14. De Lange ECM, De Bock G, Schinkel AH, De Boer AG, Breimer DD. BBB transport and P-glycoprotein functionality using MDR1A (−/−) and wild type mice. Total brain versus microdialysis concentration profiles of rhodamine-123. Pharm Res. 1998; 15:1657–1665. [PubMed: 9833984]
15. Wang Q, Yang H, Miller DW, Elmquist WF. Effect of the P-glycoprotein inhibitor, cyclosporine A, on the distribution of rhodamine-123 to the brain: an in vivo microdialysis study in freely moving rats. Biochem Biophys Res Commun. 1995; 211:719–726. [PubMed: 7598699]
16. Masereeuw R, Moons MM, Russel FGM. Rhodamine-123 accumulates extensively in the isolated perfused rat kidney and is secreted by the organic cation system. Eur J Pharmacol. 1997; 321:315–323. [PubMed: 9085043]
17. Wilson AA, Garcia A, Jin L, Houle S. Radiotracer synthesis from [^{11}C]iodomethane: a remarkably simple captive solvent method. Nucl Med Biol. 2000; 27:529–532. [PubMed: 11056365]
18. Levin VA. Relationship of octanol/water partition coefficient and molecular weight to rat brain capillary permeability. J Med Chem. 1980; 23:682–684. [PubMed: 7392035]
19. Lampidis TJ, Castello C, Del Giglio A, Pressman BC, Viallet P, Trevorrow KW, et al. Relevance of the chemical charge of rhodamine dyes to multiple drug resistance. Biochem Pharmacol. 1989; 38:4267–4271. [PubMed: 2597199]
20. Duvvuri M, Gong Y, Chatterji D, Krise JP. Weak base permeability characteristics influence the intracellular sequestration site in the multidrug-resistant human leukemic cell line HL-60. J Biol Chem. 2004; 279:32367–32372. [PubMed: 15181006]
21. Reymond F, Carrupt P-A, Testa B, Girault HH. Charge and delocalization effects on the lipophilicity of protonable drugs. Chem Eur J. 1999; 5:39–47.
22. Adhikesavalu DN, Mastropaolo D, Camerman A, Camerman N. Two rhodamine derivatives: 9-[2-(ethoxycarbonyl)phenyl]-3,6-bis-(ethylamino)-2,7-dimethylxanthylium chloride monohydrate and 3,6-diamino-9[2-(methoxycarbonyl)-phenyl]xanthylium chloride trihydrate. Acta Crystallographica. 2001; C57:657–659.
23. Zoghbi SS, Anderson KB, Jenko KJ, Luckenbaugh DA, Innis RB, Pike VW. On quantitative relationships between drug-like compound lipophilicity and plasma free fraction in monkey and human. J Pharm Sci. 2012; 101:1028–1039. [PubMed: 22170327]
24. Pfister JR, Makra F, Muehldorf AV, Wu H, Nelson JT, Cheung P, et al. Methanodibenzosuberylpiperazines as potent multidrug resistance reversal agents. Bioorg Med Chem Lett. 1995; 5:2473–2476.
25. Sweatman TW, Sehsadri R, Israel M. Metabolism and elimination of rhodamine-123 in the rat. Cancer Chemother Pharmacol. 1990; 27:205–210. [PubMed: 2265456]
26. Kannan P, Brimacombe KR, Kreisl WC, Liow JS, Zoghbi SS, Telu S, et al. Lysosomal trapping of a radiolabeled substrate of P-glycoprotein as a mechanism for signal amplification in PET. Proc Natl Acad Sci USA. 2011; 108:2593–2598. [PubMed: 21262843]
27. Rottenberg H. The measurement of membrane potential and ΔpH in cells, organelles, and vesicles. Methods Enzymol. 1979; 55:547–569. [PubMed: 37402]
28. Johnson LV, Walsh ML, Chen LB. Localization of mitochondria in living cells with rhodamine-123. Proc Natl Acad Sci USA. 1980; 77:990–994. [PubMed: 6965798]
29. Vora MM, Dhalla M. In vivo studies of unlabeled and radioiodinated rhodamine-123. Nucl Med Biol. 1992; 19:405–410.
30. Summerhayes IC, Lampidis TJ, Bernal SD, Nadakavukaren JJ, Nadakavukaren KK, Shepherd EL, et al. Unusual retention of rhodamine 123 by mitochondria in muscle and carcinoma cells. Proc Natl Acad Sci USA. 1982; 79:5292–5296. [PubMed: 6752944]
31. Meissner K, Sperker B, Karsten C, zu Schwabedissen HM, Seeland U, Bohm M, et al. Expression and localization of P-glycoprotein in human heart: effects of cardiomyopathy. J Histochem Cytochem. 2002; 50:1351–1356. [PubMed: 12364568]

32. Budde T, Haney J, Bien S, Schwebe M, Riad A, Tschope C, et al. Acute exposure to doxorubicin results in increased cardiac P-glyocoprotein expression. J Pharm Sci. 2011; 100:3951–3958. [PubMed: 21590773]
33. Gottumukkala V, Heinrich TK, Baker A, Dunning P, Fahey FH, Treves ST, et al. Biodistribution and stability studies of [^{18}F]fluoroethylrhodamine B, a potential PET myocardial perfusion agent. Nucl Med Biol. 2010; 37:365–370. [PubMed: 20346876]
34. Zhang LL, Lu L, Jin S, Jing X, Yao D, Hu N, et al. Tissue-specific alterations in expression and function of P-glycoprotein in streptozotocin-induced diabetic rats. Acta Pharmacologica Sinica. 2011; 32:956–966. [PubMed: 21685928]
35. Parasrampuria R, Mehvar R. Effects of P-glycoprotein and Mrp2 inhibitors on the hepatobiliary disposition of rhodamine-123 and its glucuronidated metabolite in isolated perfused rat livers. J Pharmaceutical Sci. 2010; 99:455–466.
36. Stapf V, Thalhammer T, Huberhuber R, Felberbauer F, Graf J. Inhibition of rhodamine-123 secretion by cyclosporine-A as a model of P-gp glycoprotein mediated transport in liver. Anticancer Res. 1994; 14:581–585. [PubMed: 7912496]
37. Martinez C, Albet C, Agundez JAG, Herrero E, Carillo JA, Marquez M, et al. Comparative in vitro and in vivo inhibition of cytochrome P450 CYP1A2, CYP2D6, and CYP3A by H_2-receptor antagonists. Clin Pharmacol Ther. 1999; 65:369–376. [PubMed: 10223772]
38. Levine M, Law EYW, Bandiera SM, Chang TKH, Bellward GD. In vivo cimetidine inhibits hepatic CYP2C6 and CYP2C11 but not CYP1A1 in adult male rats. J Pharmacol Exp Ther. 1998; 284:493–499. [PubMed: 9454789]
39. Emery S, Oldham HG, Norman SJ, Chenery RJ. The effect of cimetidine and ranitidine on paracetamol glucuronidation and sulphation in cultured rat hepatocytes. Biochem Pharmacol. 1985; 34:1415–1421. [PubMed: 3994756]
40. Clark, J.; Baldwin, R.; Bayne, K.; Brown, MJ.; Gebhart, GF.; Gonder, JC., et al. Guide for the care and use of laboratory animals. Institute for Laboratory Animal Resources, National Research Council; Washington, DC: 1996.
41. Briard E, Zoghbi SS, Imaizumi M, Gourley JP, Shetty HU, Lu S, et al. Synthesis and evaluation in monkey of two sensitive ^{11}C-labeled aryloxyanilide ligands for imaging brain peripheral benzodiazepine receptors in vivo. J Med Chem. 2008; 51:17–30. [PubMed: 18067245]
42. Gandelman MS, Baldwin RM, Zoghbi SS, Zea-Ponce Y, Innis RB. Evaluation of ultrafiltration for the free-fraction determination of single photon emission computed tomography (SPECT) radiotracers: β-CIT, IBF, and iomazenil. J Pharm Sci. 1994; 83:1014–1019. [PubMed: 7965658]
43. Zoghbi SS, Shetty HU, Ichise M, Fujita M, Imaizumi M, Liow J-S, et al. PET imaging of the dopamine transporter with ^{18}F-FECNT: a polar radiometabolite confounds brain radioligand measurements. J Nucl Med. 2006; 47:520–527. [PubMed: 16513622]

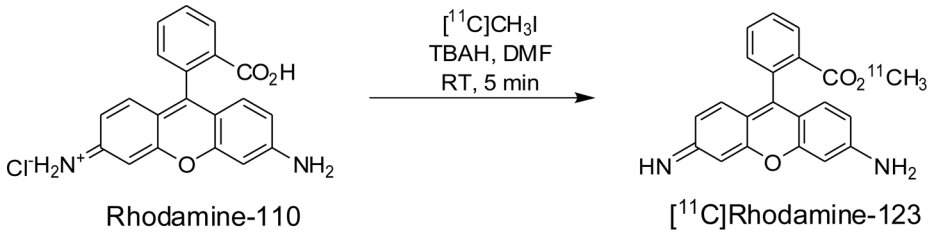

Figure 1.
Synthesis of [^{11}C]rhodamine-123.

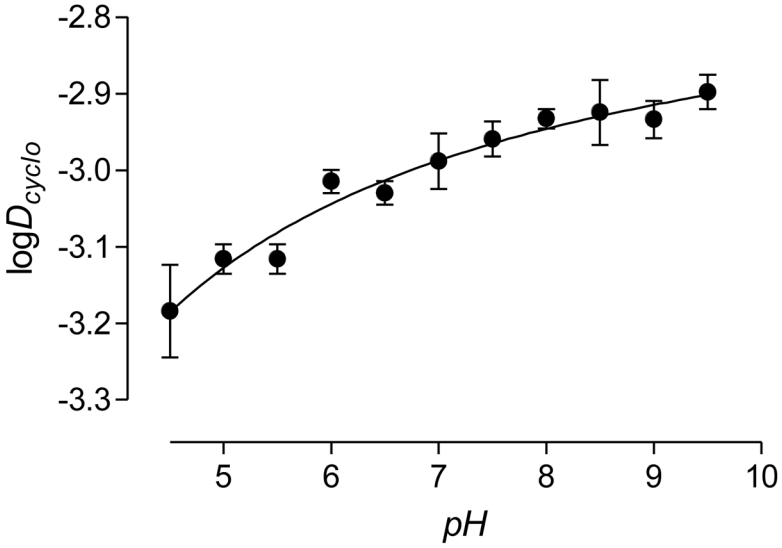

Figure 2.
pH-dependence of logD_{cyclo} for [^{11}C]rhodamine-123. Values are mean ± SD for n = 3.

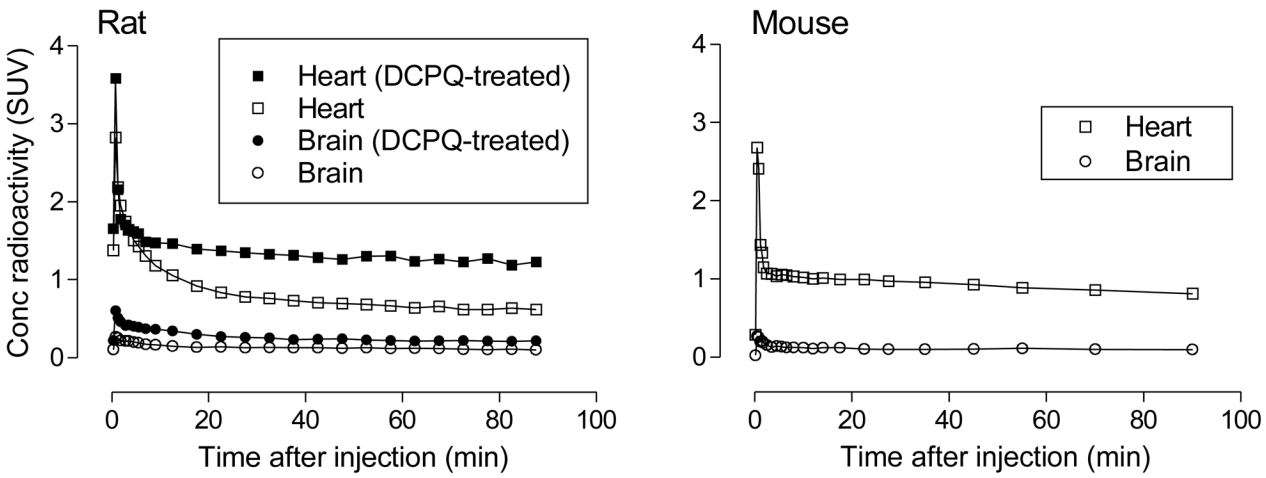

Figure 3.

PET measures of the decay-corrected time-curves for radioactivity uptake in heart and brain of rat and mouse after intravenous administration of [^{11}C]rhodamine-123. The effects of pretreatment of rats with the P-gp inhibitor, DCPQ (32 mg/kg, i.v.), are shown in the left panel.

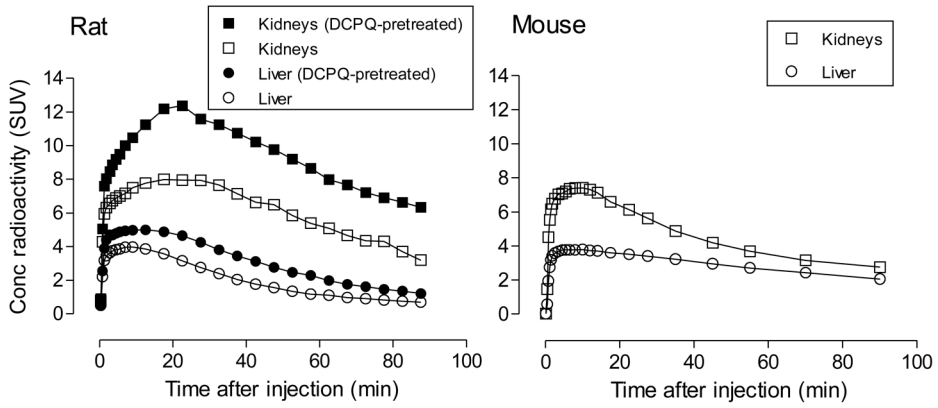

Figure 4.

PET measures of the decay-corrected time-curves of radioactivity uptake in the kidneys and liver of rat and mouse after intravenous administration of [^{11}C]rhodamine-123. The effects of pretreatment of rats with the P-gp inhibitor, DCPQ (32 mg/kg i.v.), are shown in the left panel.

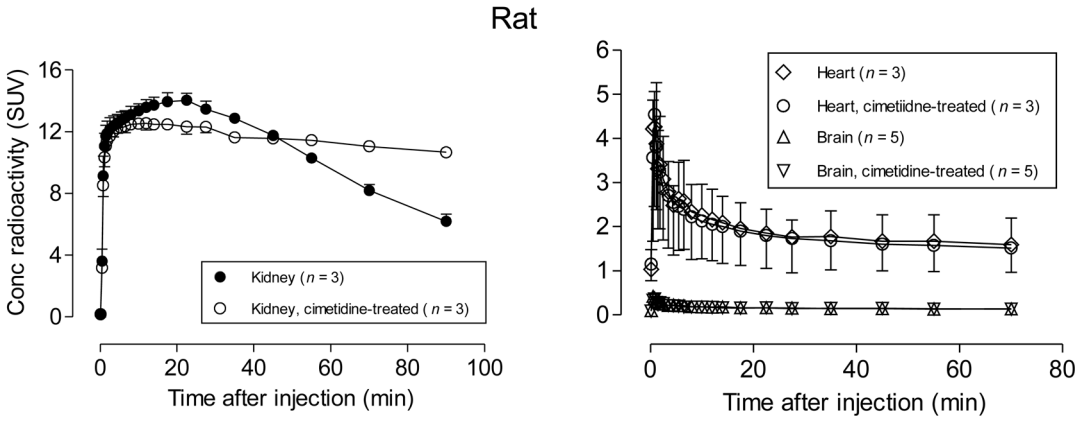

Figure 5.

PET measures of the decay-corrected time-courses of radioactivity uptake in kidney, heart and brain after intravenous administration of [^{11}C]rhodamine-123 to rats. The effects of pretreatment of rats with the OCT inhibitor, cimetidine (30 mg/kg, i.v.), are shown. Error bars represent 1 SD, and where they are not visible are within the symbol size.

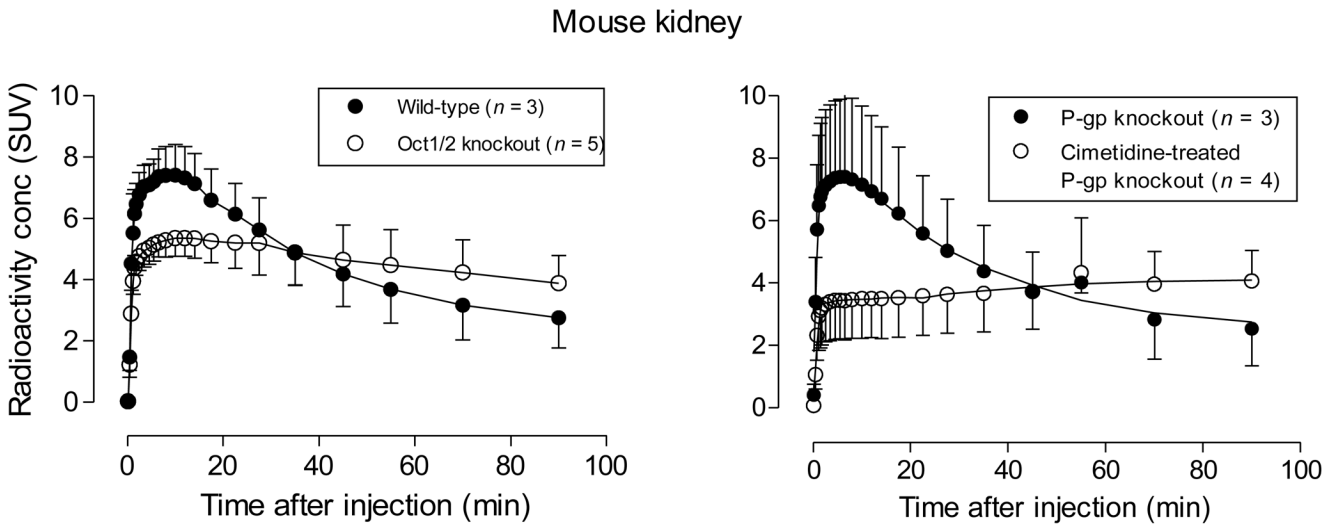

Figure 6.

PET measures of the decay-corrected time-courses of radioactivity in kidney after intravenous administration of [^{11}C]rhodamine-123 to four groups of mice: wild-type, P-gp knockout, cimetidine (30 mg/kg, i.v.) treated P-gp knockout, and Oct1/2 knockout mice. Error bars represent 1 SD.

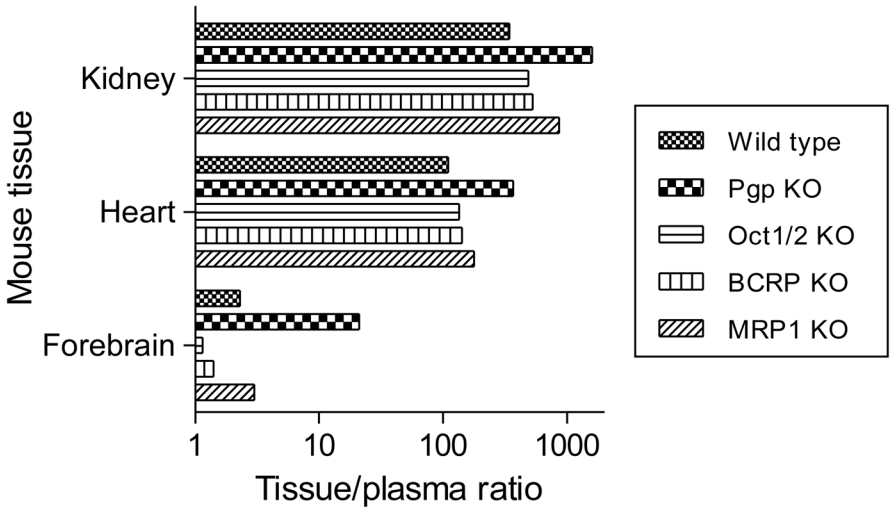

Figure 7.
Ratios of unchanged [^{11}C]rhodamine-123 in mouse tissue to that in plasma at 30 min after i.v. injection of [^{11}C]rhodamine-123 to wild-type and efflux transporter knockout mice.

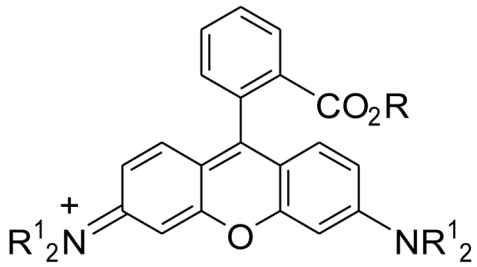

R = Me, R^1 = H; Rhodamine-123 (protonated form)
R = CH_2CH_2F, R^1 = Et; Fluoroethyl-rhodamine B

Chart 1.
Structures of rhodamine-123 and fluoroethylrhodamine B.

Table 1

Unchanged [^{11}C]rhodamine-123 in forebrain and plasma as a percentage of total organ radioactivity (mean ± SD) at 30 min after i.v. injection of [^{11}C]rhodamine-123 into untreated, DCPQ-pretreated and cimetidine-pretreated rats.

Rat tissue	Radioactivity content represented by unchanged [^{11}C]rhodamine-123 (%)		
	Untreated (n = 3)	DCPQ-pretreated (n = 3)	Cimetidine-pretreated (n = 3)
Forebrain	68.1 ± 9.2	77.7 ± 5.9	80.4 ± 7.7
Plasma	79.7 ± 7.1	57.3 ± 8.8	94.2 ± 2.4

Table 2

Concentrations (SUV; mean ± SD) of unchanged [^{11}C]rhodamine-123 in forebrain and plasma at 30 min after i.v. injection of [^{11}C]rhodamine-123 into untreated, DCPQ-pretreated and cimetidine-pretreated rats.

Rat tissue	Concentration of unchanged [^{11}C]rhodamine-123 (SUV)		
	Untreated (*n* = 3)	DCPQ-pretreated (*n* = 3)	Cimetidine-pretreated (*n* = 3)
Forebrain	0.044 ± 0.015	0.053 ± 0.021	0.040 ± 0.012
Plasma	0.30 ± 0.112	0.098± 0.018	0.473 ± 0.059

Table 3

Unchanged [^{11}C]rhodamine-123 in various organs as a percentage of total organ radioactivity (mean ± SD) at 30 min after i.v. injection of [^{11}C]rhodamine-123 into wild-type and efflux transporter knockout mice.

Mouse tissue	Radioactivity content represented by unchanged [^{11}C]rhodamine-123 (%)				
	Wild-type (*n* = 3)	**P-gp KO (*n* = 3)**	**Oct1/2 KO (*n* = 3)**	**BCRP KO (*n* = 4)**	**MRP1 KO (*n* = 3)**
Plasma	14.3 ± 13.4	4.1 ± 2.3	12.8 ± 1.7	14.7 ± 4.3	7.5 ± 3.9
Forebrain	82.3 ± 4.3	85.8 ± 6.0	38.1 ± 15.2	48.1 ± 14.2	73.3 ± 6.2
Heart	97.0 ± 3.9	97.8 ± 1.2	98.6 ± 0.2	98.5 ± 0.3	99.4 ± 0.1
Kidney	98.9 ± 0.5	97.6 ± 1.9	98.4 ± 0.5	98.3 ± 0.2	99.2 ± 0.3

Table 4

Concentrations (SUV; mean ± SD) of unchanged [^{11}C]rhodamine-123 in plasma, forebrain, heart and kidney at 30 min after i.v. injection of [^{11}C]rhodamine-123 into wild-type and efflux transporter knockout mice.

Mouse tissue	Unchanged [^{11}C]rhodamine-123 concentration (SUV)				
	Wild-type (*n* = 3)	**P-gp KO (*n* = 3)**	**Oct1/2 KO (*n* = 3)**	**BCRP KO (*n* = 4)**	**MRP1 KO (*n* = 3)**
Plasma	0.031 ± 0.032	0.008 ± 0.004	0.026 ± 0.003	0.022 ± 0.008	0.014 ± 0.007
Forebrain	0.071 ± 0.025	0.168 ± 0.008	0.029 ± 0.011	0.031 ± 0.015	0.042 ± 0.005
Heart	3.40 ± 0.69	2.95 ± 0.29	3.51 ± 0.41	3.13 ± 1.66	2.51 ± 0.013
Kidney	10.7 ± 2.23	12.8 ± 4.9	12.7 ± 0.12	11.7 ± 3.87	12.1 ± 2.35